ISSN 0016-7029, Geochemistry International, 2024, Vol. 62, No. 7, pp. 733–747. © Pleiades Publishing, Ltd., 2024.
ISSN 0016-7029, Geochemistry International, 2024. © Pleiades Publishing, Ltd., 2024.

The Timing and Genesis of Late Paleoproterozoic Molybdenum Mineralization in the East Qinling Molybdenum Belt, China: Constraints from the Zhaiwa Deposit

Bing Yu[a, b], Qingdong Zeng[c, d], Shuai Gao[e], Jianling Xue[a, b, *], and Xiaofei Zhang[a, b]

[a] *Development and Research Center, China Geological Survey, Beijing, 100037 China*

[b] *Mineral Exploration Technical Guidance Center, Ministry of Natural Resources, Beijing, 100037 China*

[c] *Key Laboratory of Mineral Resources, Institute of Geology and Geophysics, Chinese Academy of Sciences, Beijing, 100029 China*

[d] *College of Earth and Planetary Sciences, University of Chinese Academy of Sciences, Beijing, 100049 China*

[e] *MNR Key Laboratory of Gold Mineralization Processes and Resources Utilization, Key Laboratory of Metallogenic-Geologic Processes and Comprehensive Utilization of Minerals Resources of Shandong Province, Shandong Institute of Geological Sciences, Jinan, 250013 China*

**e-mail: xjianling@mail.cgs.gov.cn*

Received November 23, 2023; revised March 9, 2024; accepted April 5, 2024

Abstract—The East Qinling Molybdenum Belt (EQMB), which is located on the southern margin of the North China Craton (NCC), is the largest Mo province in the world. This belt hosts a significant number of Mesozoic magmatic-hydrothermal Mo deposits and a small portion of pre-Mesozoic Mo deposits. Understanding the mineralization timing and mechanism of the unique pre-Mesozoic Mo deposits is essential to comprehend the evolution of the EQMB, the pre-Mesozoic Mo enrichment, and the Mesozoic Mo mineralization event. The recently discovered Zhaiwa deposit is a porphyry Mo deposit located in the Xiong'er Terrane of the EQMB. In this study, five molybdenite samples from the Mo-bearing quartz veins were analyzed for Re-Os isotopes composition. These samples yield an isochron age of 1794 ± 45 Ma, which represents the age of mineralization. The mineralization is mostly hosted within the biotite-amphibole plagiogneiss and granite porphyry. LA-ICP-MS U-Pb data of zircons constrain the crystallization age of the granite porphyry to be at 1791 ± 16 Ma. The close spatial and temporal association suggests that the granite porphyry is the causative rocks of the Mo mineralization. The $\delta^{34}S$ values of pyrite vary from 5.3 to 6.8‰, suggesting that the S was mainly derived from magmatic source. The intrusion of magmas and associated Mo mineralization are contemporaneous to the regional Xiong'er volcanism that occurred during the late Paleoproterozoic. The Xiong'er volcanism was triggered by partial melting of lithospheric mantle in an extensional setting. The results of our study provide robust evidence for a late Paleoproterozoic Mo metallogenic event along the southern margin of the NCC. Future exploration should also consider the potential of late Paleoproterozoic porphyry Mo mineralization existing in the EQMB, which is closely associated with the Xiong'er volcanism.

Keywords: molybdenite Re–Os age, zircon U-Pb age, sulfur isotope, Zhaiwa Mo deposit, Xiong'er volcanism, East Qinling Mo Belt

DOI: 10.1134/S0016702924700381

INTRODUCTION

Molybdenum has the characteristics of high strength and melting point, as well as corrosion and wear resistance, so it readily forms hard, stable carbides in alloys, and for this reason most molybdenum produced is used in metallurgy, with the rest used in chemical applications as pigments and catalysts (Shields and Baker, 1999; Liu et al., 2013). China has the largest molybdenum resource and is also the largest molybdenum producer in the world, with the majority being concentrated in the East Qinling Molybdenum Belt (EQMB) (Li et al., 2007; Chen et al., 2017a), Northeast China (Chen et al., 2017b), Northwest China (Wu et al., 2017), Southwest China (Yang and Wang, 2017), and South China (Wang et al., 2022). The EQMB is located on the southern margin of the North China Craton (NCC), is the most significant Mo province in China, with accumulated proven Mo reserves of >8.9 Mt (Zeng et al., 2013). Previous studies have suggested that most of the Mo deposits in the EQMB are related to Mesozoic porphyry/skarn systems (Hu et al., 1988; Stein et al., 1997; Chen et al., 2000; Zhou et al., 2020; Hu et al., 2022). However, a geochronology study has constrained the existence of two dominant episodes of Mesozoic Mo mineraliza-

tion in the EQMB, namely Triassic and Late Jurassic–Early Cretaceous (Mao et al., 2008, 2011).

In addition, several pre-Mesozoic Mo deposits were identified in the region, including the Zhaiwa porphyry Mo deposit and the Longmengdian quartz-vein type Mo deposit (Deng et al., 2009; Li et al., 2009, 2011a). The pre-Mesozoic Mo deposits in the EQMB carry unique characteristics, forming during the Paleoproterozoic and spatially in close association with the Xiong'er Terrane. In contrast to the Mesozoic Mo deposits, few works were carried out to enable understanding of the geological significance of the Paleoproterozoic Mo mineralization and the geodynamic background. The knowledge of the timing and formation mechanisms of the unique pre-Mesozoic Mo deposits is crucial to understand the evolution of the EQMB and the pre-Mesozoic Mo enrichment (Hu et al., 1988; Chen et al., 2000).

The Zhaiwa porphyry Mo deposit is well studied since its discovery after 2000. Previous work have reported the geological characteristics (Li et al., 2009; Yang et al., 2003a, 2003b; Liu et al., 2004), isotope geochemistry (Deng et al., 2013a, 2013b; Li et al., 2023), the nature of ore-forming fluids (Deng et al., 2008), and the timing of Mo mineralization (Deng et al., 2009; Li et al., 2009). However, the classification of the Zhaiwa deposit was controversial, such as: (1) orogenic Mo deposit (Chen, 2006); (2) intrusion-related Mo deposit (Deng et al., 2008); and (3) porphyry Mo deposit (Deng et al., 2013a, 2013b). In many instances, porphyry deposits in the upper crust are spatially and genetically related to intermediate and silicic hypabyssal porphyritic intrusive rocks (Kirkham, 1972). For the Zhawai porphyry Mo deposit, however, identification of the causative porphyry body is still absent. This is largely due to a lack of systematic comparison of the timing of Mo mineralization to the regional magmatic rocks. To address this question, we conducted detailed field observation and identified the intrusions that are spatially associated with the Mo orebodies. A molybdenite Re-Os isochron age and a zircon U-Pb age are reported in this study are suggested to represent the formation ages of Mo mineralization and the spatially associated intrusion (granite porphyry), respectively. In situ S isotope analysis of pyrite from the quartz-polymetallic sulfide vein is applied to constrain sulfur source in the Zhawai deposit. Built upon the geochronological evidence, the geological context of Zhaiwa was further considered to infer the geodynamic setting that are responsible for the Paleoproterozoic Mo mineralization in the EQMB, and its implication for future exploration in the region.

REGIONAL GEOLOGY

The EQMB is located between the NCC and the Yangtze Craton (Fig. 1a). This metallogenic belt is notable for Au, Ag, Pb, Zn, Mo, W, and REE resources (Xie et al., 2001; Mao et al., 2002; Chen et al., 2006; Li et al., 2008; Feng et al., 2022), and is the most significant Mo province in China (Zeng et al., 2013; Mao et al., 2008, 2011). It is part of the 2000-km-long Qinling-Dabie orogen, which was formed by the collision between the NCC and the Yangtze Craton during the Mesozoic (Chen et al., 2009; Dong et al., 2011). It is bounded by the San-Bao Fault to the north and is separated from the North Qinling orogenic belt by the Luanchun Fault in the south (Fig. 1b). The Xiong'er Terrane is one of the representative regions in the EQMB. The boundaries of the Xiong'er Terrane are the San-Bao Fault to the north and the Machaoying Fault to the south (Fig. 1c).

The main lithostratigraphic units of the Xiong'er Terrane are the Taihua Supergroup (basement) and the Xiong'er Group (cover). The Taihua Supergroup comprises a suite of medium- to high grade metamorphic rocks (Zhang et al., 1985), including late Archean tonalitic-trondhjemitic-granodioritic (TTG) gneisses and Paleoproterozoic amphibolite- and granulite-facies metamorphic rocks (Kröner et al., 1988; Xue et al., 1995; Zhang et al., 2001). The Taihua Supergroup has been subdivided into the Beizi, Dangzehe, and Shuidigou groups (Chen and Zhao, 1997). The Xiong'er Group, which crops out over an area of more than 60000 km^2 (Zhao et al., 2009), is a well-preserved unmetamorphosed volcanic sequence that unconformably overlies the Taihua Supergroup. The Xiong'er Group is composed predominantly of lavas and pyroclastic rocks intercalated with minor sedimentary rocks (<5%) and has been subdivided, from bottom to top, into four formations: the Dagushi, Xushan, Jidanping, and Majiahe ones (Zhao et al., 2009). Recent zircon U-Pb age data show that the eruption of the Xiong'er volcanic rocks was concentrated between 1.85 and 1.73 Ga, with the peak occurring at 1.78–1.75 Ga (Zhao et al., 2009; He et al., 2009; Wang et al., 2010a; Cui et al., 2011). However, the origin of the volcanic event is still controversial with highly variable explanations. An arc setting was proposed in relation to the north-dipping oceanic plate subduction beneath the NCC (Hu et al., 1988; Jia, 1987; Chen and Fu, 1992); a continental rift setting (Sun et al., 1981, 1985) or mantle plume (Peng et al., 2008) causing the breakup of the Columbia supercontinent; and more recently, a tectonic setting of flat subduction model for the plate-margin magmatism in the late Archean (Wang et al., 2010a).

The Xiong'er Terrane is characterized by a series of approximately parallel NE–SW-trending faults on the northern side of the Machaoying Fault (Fig. 1c). These faults include, from east to west, the Taocun-Mayuan, Hongzhuang-Qinggangping, Kangshan-Qiliping, and Sanmen-Tieluping faults, all of which are secondary to the development of the E–W-trending Machaoying Fault. Detailed structural analysis reveals that the NE–SW-trending faults result from early compression, followed by late extensional shearing in a tensional regime (Chen et al., 2009; Chen and

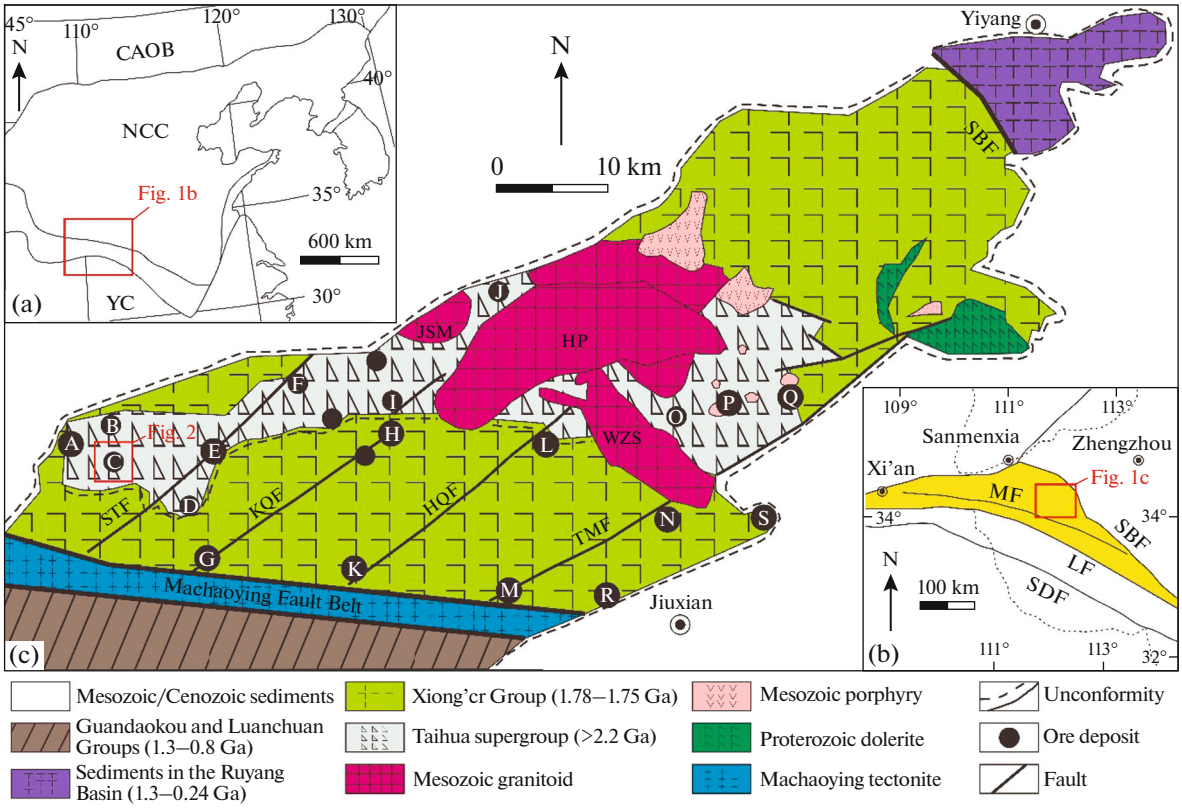

Fig. 1. (a) Regional-scale tectonic framework of the EQMB; (b) simplified tectonic framework of the EQMB; (c) simplified geologic map of the Xiong'er Terrane showing the location of ore deposits including the Zhaiwa deposit (modified from Li et al., 2011a; Deng et al., 2013a; Chen et al., 2004). Abbreviations: CAOB, Central Asian Orogenic Belt; NCC, North China Craton; YC, Yangtze Craton; SBF, San–Bao Fault; MF, Machaoying Fault; LF, Luanchuan Fault; SDF, Shang–Dan Fault; STF, Sanmen–Tieluping Fault; KQF, Kangshan–Qiliping Fault; HQF, Hongzhuang–Qinggangping Fault; TMF, Taocun–Mayuan Fault; JSM, Jinshanmiao granite; HP, Haoping granite; WZS, Wuzhangshan granite. Ore deposits: A, Shagou Ag-Pb-Zn; B, Haopinggou Ag-Pb; C, Zhaiwa Mo; D, Longmendian Mo; E, Tieluping Ag-Pb; F, Xiaochigou Au; G, Kangshan Au-Ag-Pb; H, Shanggong Au; I, Hugou Au; J, Shapoling Mo; K, Hongzhuang Au; L, Qinggangping Au; M, Tantou Au; N, Yaogou Au; O, Huangshui'an Mo; P, Leimengou Mo-Au; Q, Qiyugou Au; R, Qianhe Au; S, Zhifang Mo.

Zhao, 1997). The E–W-trending Machaoying Fault, which extends for more than 200 km and has an inferred depth of 34–38 km, was reactivated as a strike-slip fault in the late Mesozoic (Zhang et al., 2001). This later fault underwent at least two major deformational stages, including an early ductile deformation characterized by thrusting from north to south and subsequent overprinting by late brittle faulting (Han et al., 2009).

The occurrence of late Paleoproterozoic intrusions in the Xiong'er Terrane includes granite porphyry, diorite porphyrite, quartz diorite, and dolerite. For instance, the Shizhaigou quartz diorite and the Luoling granite porphyry, which intruded into the Majiahe Formation of the upper part of the Xiong'er Group, has yielded zircon $^{207}Pb/^{206}Pb$ ages of 1778 ± 12 Ma and 1786 ± 8 Ma (Cui et al., 2010), respectively. The two lithostratigraphic units of the Xiong'er Terrane are subsequently intruded by the Mesozoic (Jurassic–Cretaceous) granitoids (Fig. 1c), including the Huashan granitic complex (Jinshanmiao, Haoping, and Wuzhangshan granites), abundant mineralized porphyries, diatremes, and breccia pipes (Chen et al., 2009; Fan et al., 2000, 2011; Li et al., 2012; Qian et al., 2023).

DEPOSIT GEOLOGY

The Zhaiwa Mo deposit (34°08′47″ N, 111°16′55″ E) is located at the junction of Luoning county and Lushi county, Henan Province. Copper-bearing veins were first discovered at the deposit, and the Cu grade is between 2.4 and 14.3%. The deposit was thus initially defined to be a large-tonnage porphyry-type Cu (-Ag–Au) deposit (Yang et al., 2003a, 2003b). Continued prospecting has proven that Mo can be more economic Cu, and that the deposit can be regarded as a Mo-dominated polymetallic system. The deposit lies within the Shibangou Formation comprises of the Taihua Supergroup in the Xiong'er Terrane (Fig. 2) and has Mo reserves of >0.1 Mt with an average grade of 0.064% Mo (Li et al., 2009; Deng et al., 2013a). The Shibangou Formation of biotite-amphibole plagiogneiss, and minor biotite plagiog-

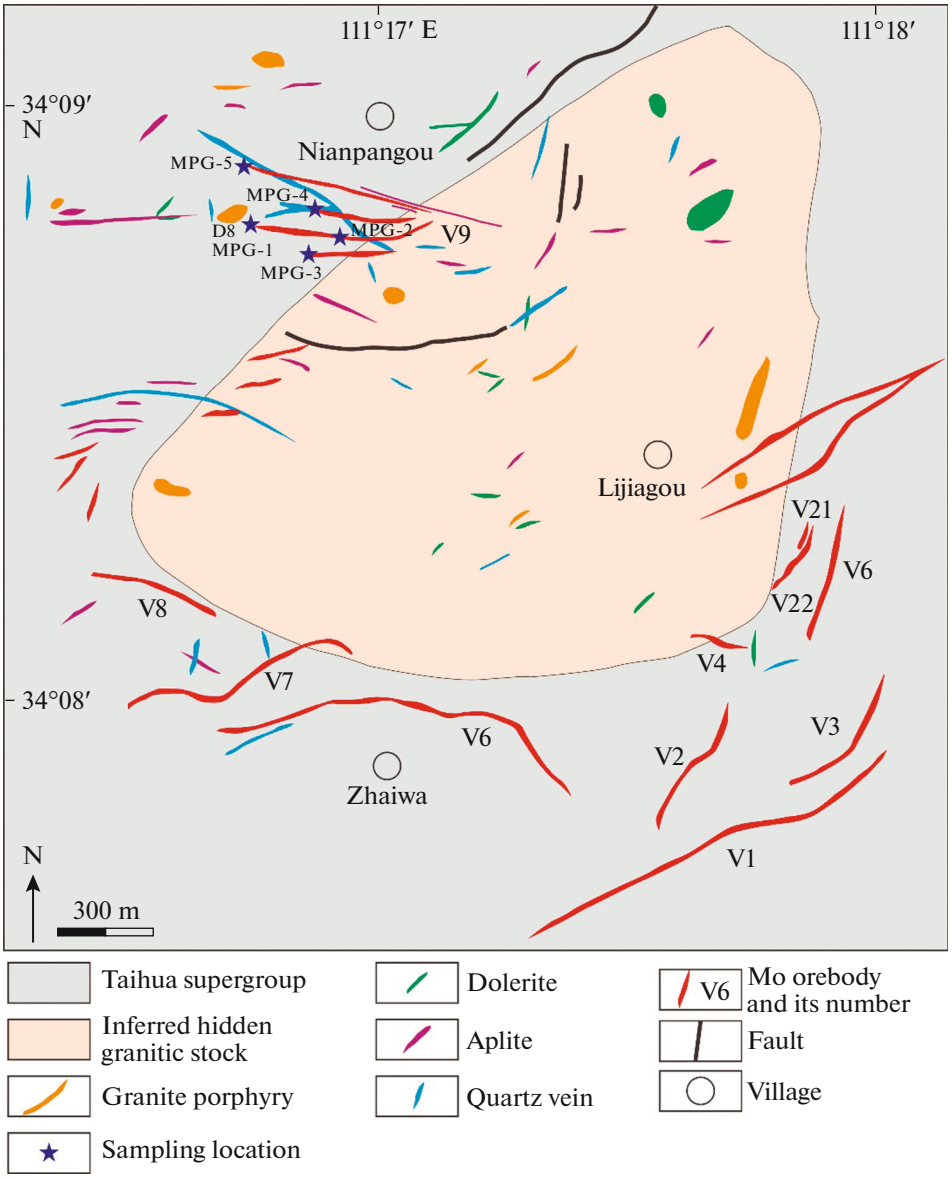

Fig. 2. Geological map of the Zhaiwa Mo deposit (modified from Deng et al., 2013a).

neiss and amphibole plagiogneiss (Deng et al., 2008). The Mo orebodies commonly occur as lodes associated with faults bounding to a hidden granitic stock (Fig. 2) inferred from geophysical evidence such as low gravity and weak magnetism (Liu et al., 2004; Wang et al., 1997). Most of the Mo-bearing quartz veins are hosted within the biotite-amphibole plagiogneiss (Figs. 3a–3e) and aplite, while the Mo-bearing quartz veinlets tend to occur within the granite porphyry dikes (Fig. 3f). The NNE-, NE- and EW-trending granite porphyry dikes are sporadically developed in the deposit (Fig. 2), ranging from 0.5 to 10 m in width and tens to hundreds of meters in length. Most of the orebodies have lengths of several hundred meters and thicknesses of 2–15 m, striking ENE–WSW, and dipping to the NW at angles of 58°–80°.

The major orebodies are hosted by quartz veins and are referred to V1, V5, V6, V7, V9, V21, and V22 orebodies (Fig. 2). The Mo mineralization mainly occurs in lodes, with lesser proportions of brecciated, disseminated and banded Mo-ores occurring in stockworks (Figs. 3a–3f). The principal ore minerals are molybdenite (Figs. 3g–3i) and pyrite, together with minor chalcopyrite, sphalerite, galena, pyrrhotite, bismuthinite, and native bismuth. The gangue minerals include quartz, and minor K-feldspar, muscovite, fluorite (Fig. 3c), calcite, chlorite, and epidote. Most of the molybdenite occurs in disseminations in the hydrothermal quartz veins and shows leaf-like and scale-like habits. The crystal size of molybdenite is generally between 2 and 9 mm, with a maximum of 4 cm. The mineralization at Zhaiwa can be divided into three

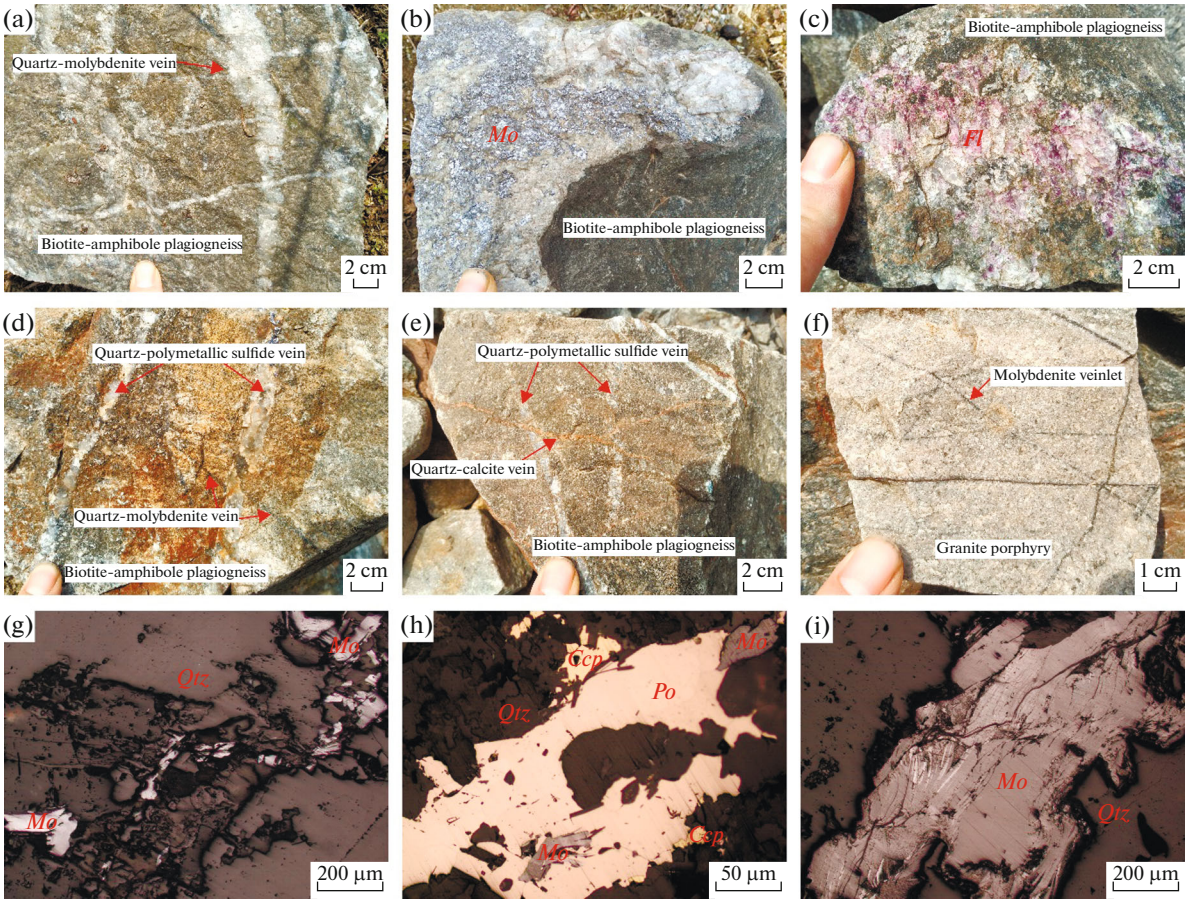

Fig. 3. Representative photomicrographs of thin sections (a–f) and photographs of hand specimens (g–i) from the Zhaiwa porphyry Mo deposit. (a) Stockwork Mo mineralization hosted by biotite-amphibole plagiogneiss; (b) thin layer of molybdenite in quartz-molybdenite vein; (c) quartz-fluorite vein; (d) quartz-polymetallic sulfide vein cutting quartz-molybdenite vein; (e) quartz-calcite vein cutting quartz-polymetallic sulfide vein; (f) molybdenite veinlet hosted by granite porphyry; (g) molybdenite within a quartz veinlet; (h) sulfides from a quartz-polymetallic vein, including molybdenite, pyrrhotite, and chalcopyrite; (i) lepidosome molybdenite. Abbreviations: *Ccp*, chalcopyrite; *Fl*, fluorite; *Mo*, molybdenite; *Po*, pyrrhotite; *Qtz*, quartz.

hydrothermal stages (Deng et al., 2013a) based on paragenetic assemblages and crosscutting relationships (Figs. 3d–3e): an early quartz-molybdenite stage, an intermediate quartz-polymetallic sulfide stage, and a late quartz-calcite stage.

The Mo mineralization is associated with pervasive wall-rock alteration dominated by silicification, K-feldspathization, sericitization, chloritization, epidotization, carbonation, and fluoritization.

SAMPLING AND ANALYTICAL METHODS

Samples

All the samples used for this study were collected from adit tunnels in the Zhaiwa deposit, close to the village of Nianpangou (Fig. 2). Zircon grains were separated from the granite porphyry host rock (sample D8) and selected for U-Pb dating to constrain the crystallization age. The granite porphyry is medium to fine grained and is composed of phenocrysts of K-feldspar (15%) and quartz (10%) in a matrix of plagioclase and biotite, with accessory zircon, monazite, apatite, magnetite, ilmenite and xenotime.

Five samples of molybdenite were collected from the Mo-bearing quartz veins for Re–Os dating. The molybdenite occurs as euhedral molybdenite crystals without clay intergrowths. Two samples representative of the intermediate quartz-polymetallic sulfide stage were selected for in situ S isotope analysis of pyrite.

Analytical Methods

Zircon grains selected for U-Pb analysis were mounted in epoxy resin, and then polished and imaged using reflected light, transmitted light, and cathodoluminescence (CL). Zircon U-Pb analyses were performed by laser ablation inductively coupled plasma mass spectroscopy (LA-ICP-MS) at the Wuhan Sample Solution Analytical Technology Co., Ltd., Wuhan, China. Analyses were performed on a quadrupole ICP-MS instrument (Agilent 7700) coupled with a 193 nm ArF excimer laser ablation system

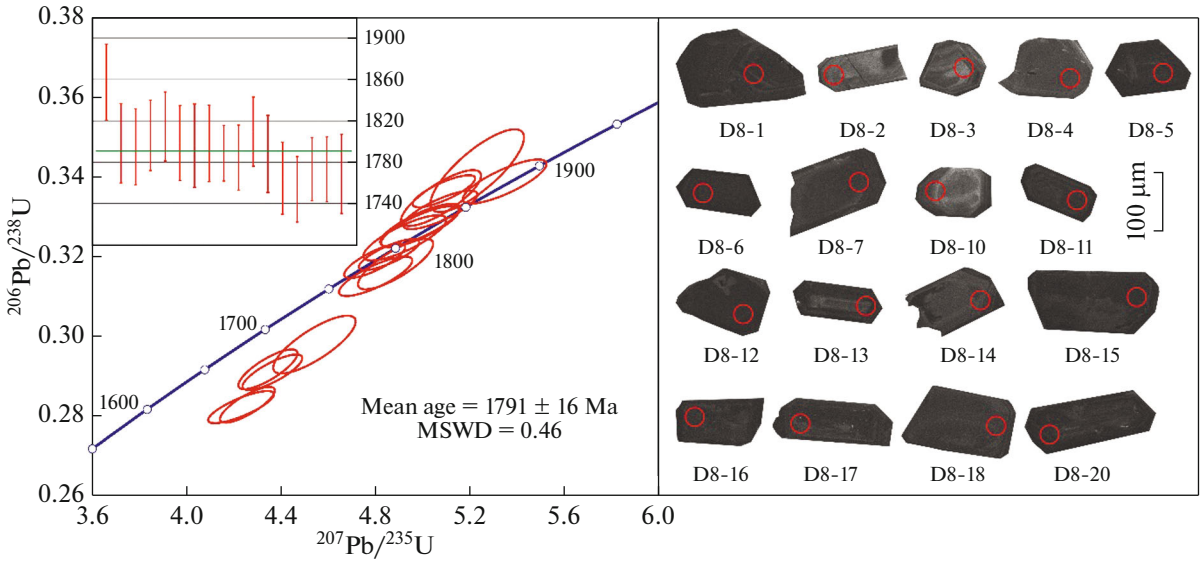

Fig. 4. Zircon U-Pb concordia diagram and CL images of granite porphyry from the Zhaiwa Mo deposit. The red circles in the CL images represent the sites for the LA-ICP-MS U-Pb analyses.

(GeoLasPro). The beam diameter was 32 μm, the laser energy density was 10 J/cm^2, and the repetition rate was 5 Hz. Details of the analytical procedures used during LA-ICP-MS zircon U-Pb dating are described by Liu et al. (2010). Zircon analyses were calibrated against the NIST SRM 610 glass external standard, and Si was used as an internal standard. Zircon standard 91500 was also used as an external standard for the U-Pb dating and was analyzed twice after every six analyses. Quantitative calibration for the U-Pb dating was performed using ICPMSDataCal software (Liu et al., 2010). Isoplot/Ex ver. 3.00 software was used to construct concordia diagrams and perform calculations of weighted mean ages (Ludwig, 2003). The analytical data are presented on U-Pb concordia diagrams. The uncertainties are 1σ, and the mean ages are weighted means with a confidence level of 95%.

Molybdenite was separated from five samples using a binocular microscope. Magnetic separation of the selected material yielded fresh unoxidized molybdenite grains measuring 0.1 mm in diameter. Re–Os isotope analyses were conducted at the Re–Os Laboratory, National Research Center of Geoanalysis, Chinese Academy of Geological Sciences, Beijing, China. The concentrations of Re, ^{187}Re, and ^{187}Os were measured using a TJA X-series ICP-MS instrument. A Carius tube (a thick-walled borosilicate glass ampoule) digestion was used. Chemical separation and mass spectrometry of Re–Os followed the procedures described by Du et al. (2004) and Zhou et al. (2012). The average Re and Os blanks for the total Carius tube procedure were less than 10 and 1 pg, respectively. The analytical reliability was tested by repeated analyses of the molybdenite standard HLP from a carbonatite vein-type Mo–Pb deposit in the Jinduicheng–Huanglongpu area of Shanxi Province, China (Stein et al., 1997). The uncertainty on each individual age determination, including the uncertainties in the decay constant of ^{187}Re, isotope ratio measurements, and spike calibrations, was approximately 1.4%. The Re–Os model age is calculated as $t = 1/\lambda\,[\ln(1 + {}^{187}Os/{}^{187}Re)]$, where λ is the decay constant of ^{187}Re ($\lambda = 1.666 \times 10^{-11}$ year^{-1}) (Smoliar et al., 1996). Concordia diagrams and weighted mean calculations were made using Isoplot/Ex ver. 3.00 software (Ludwig, 2003). All uncertainties (2δ) are given as absolute amounts at the 95% confidence level.

In situ S isotope analysis of pyrite was performed using a Neptune Plus MC-ICP-MS that is coupled with a RESOlution SE 193 nm New Wave Ar-F Excimer laser ablation system at the Beijing Createch Testing Technology Co., Ltd., Beijing, China. Pyrite was analyzed using a fluence of 3.02 J/cm^2, a repetition rate of 3 Hz, and a beam diameter of 20 μm. The standard-sample bracketing was used to determine the $\delta^{34}S$ values of each pyrite during the analysis. The external standard for pyrite (ZX, 16.9‰) was used to calibrate the instrumental mass bias during the analysis. For the detailed analytical procedure see Yu et al. (2024). The analytical precision (2σ) was found to be better than 0.2‰.

RESULTS

Zircon U-Pb Age

Most of the zircon grains are prismatic, transparent to sub-transparent and colorless, and 100 to 250 μm in size with aspect ratios between 1 : 1 and 3 : 1. Zircon grains commonly display oscillatory and planar zoning in CL images; these features are typical of magmatic zircons (Fig. 4). Uranium concentrations are

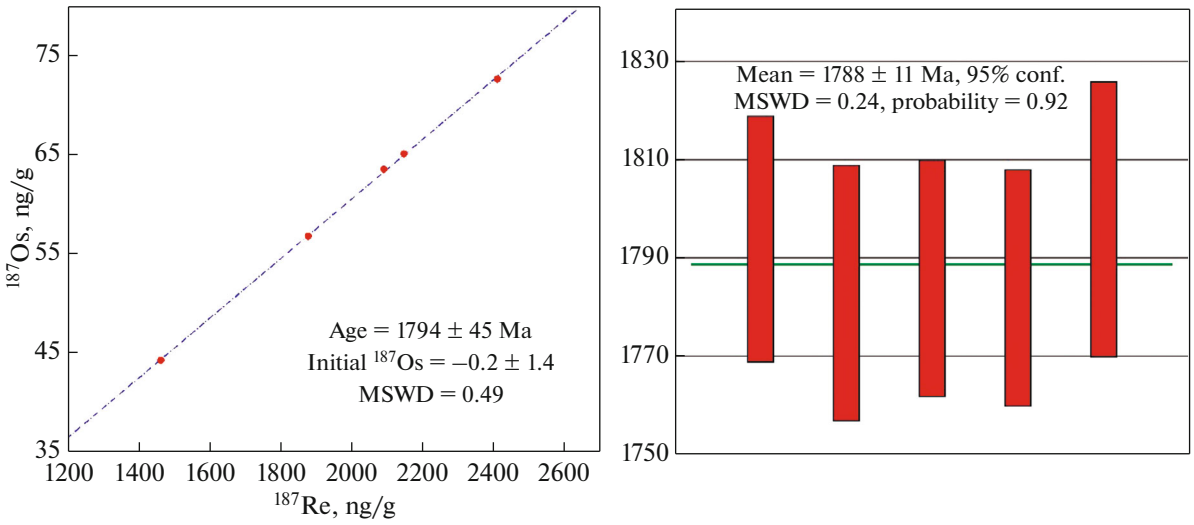

Fig. 5. Re–Os isochron and weighted mean model ages of molybdenite samples from the Zhaiwa Mo deposit.

between 750 and 12845 ppm, and Th concentrations are between 459 and 7368 ppm (Table 1). Th/U ratios vary from 0.283 to 0.725, consistent with a magmatic origin (Hoskin and Black, 2000). Most of the results plot close to the concordia curve (Fig. 4). Seventeen spots were analyzed on grains from the granite porphyry, yielding concordant ^{207}Pb/^{206}Pb ages with a weighted mean age of 1791 ± 16 Ma (MSWD = 0.46), which is interpreted as the age of magmatic crystallization and the emplacement age of the granite porphyry dike.

Molybdenite Re-Os Age

Total Re concentrations of the five samples are between 2330 and 3834 ppb (Table 2). The total ^{187}Re and ^{187}Os concentrations are between 1464 and 2410 ppb and 44.22 and 72.63 ppb, respectively. The ^{187}Re and ^{187}Os concentrations vary for each of the five samples and yield an isochron age of 1794 ± 45 Ma (2σ, MSWD = 0.49) with initial ^{187}Os of –0.2 ± 1.4 ppb (Fig. 5). The Re-Os model ages display a narrow range between 1798 and 1783 Ma (Fig. 5), with a weighted mean age of 1788 ± 11 Ma. The isochron age is consistent with the model ages for individual samples (Table 2). Within error, the molybdenite Re-Os isochron age lies close to the zircon U-Pb age of the granite porphyry dike (1791 ± 16 Ma, this study). The combined data suggest that the Mo mineralization at the Zhaiwa deposit is related to emplacement of the ore-bearing granite porphyry.

In Situ Sulfur Isotope Data

A total of 15 S isotope measurements of pyrite from the intermediate quartz-polymetallic sulfide stage are presented in Table 3. The δ^{34}S values of pyrite range from 5.3 to 6.8‰, with a mean of 6.0‰.

DISCUSSION

Chronological Relationships between Magmatism and Mineralization

The Re–Os molybdenite geochronometer has been shown to be unaffected by intense deformation and metamorphism (Stein et al., 1998). If molybdenite does not contain any initial or common Os, all measured Os is monoisotopic (^{187}Os) produced by ^{187}Re decay, then the isochron age represents the age of formation of the molybdenite (Suzuki et al., 1996; Brenan et al., 2000; Barra et al., 2003). At Zhaiwa, the five molybdenite samples yield an isochron age of 1794 ± 45 Ma (2σ, MSWD = 0.49) with an initial ^{187}Os of –0.2 ± 1.4 ppb, indicating that the Zhaiwa Mo mineralization in the EQMB was formed during the late Paleoproterozoic.

In the field, we observed that Mo mineralization is closely spacially associated with the granite porphyry dikes, and the deposit is characterized by classic porphyry-style stockworks, quartz veins, and disseminations (Figs. 3a, 3b). Wall-rock alteration associated with the Mo mineralization is typical of that in classic porphyry Mo systems and includes silicification, K-feldspathization, sericitization, chloritization, epidotization, carbonation, and fluoritization. Field observations show that Mo-bearing quartz veinlets occasionally crosscut the granite porphyry (Fig. 3f) and that the quartz veinlets postdate the granite porphyry dike. It is therefore reasonable to conclude that the Mo mineralization occurred after the emplacement of the granite porphyry. The zircon U-Pb age of the granite porphyry is 1791 ± 16 Ma, which represents the time of magma emplacement. The similar ages for Mo mineralization and granite porphyry emplacement suggest that the two events were synchronous and genetically related. In many instances, porphyry magmas are fertile of providing ore-forming materials

Table 1. LA-ICP-MS zircon U-Pb isotopic dating of granite porphyry from the Zhaiwa Mo deposit

Spots	Concentrations, ppm			Isotope ratio						Age, Ma					
	^{232}Th	^{238}U	Th/U	$^{207}Pb/^{206}Pb$	1σ	$^{207}Pb/^{235}U$	1σ	$^{206}Pb/^{238}U$	1σ	$^{207}Pb/^{206}Pb$	1σ	$^{207}Pb/^{235}U$	1σ	$^{206}Pb/^{238}U$	1σ
D8-1	2362	4623	0.511	0.11354	0.00238	5.35	0.12	0.33886	0.00365	1857	37	1877	19	1881	18
D8-2	665	1051	0.632	0.10983	0.00229	4.80	0.10	0.31510	0.00327	1798	38	1785	18	1766	16
D8-3	459	812	0.565	0.10974	0.00221	4.99	0.11	0.32757	0.00339	1795	37	1818	19	1827	16
D8-4	610	1052	0.580	0.11040	0.00213	5.08	0.10	0.33174	0.00318	1806	34	1832	17	1847	15
D8-5	3474	5252	0.661	0.11091	0.00204	4.89	0.11	0.31816	0.00418	1815	33	1800	18	1781	20
D8-6	3029	10719	0.283	0.10995	0.00216	4.54	0.12	0.29795	0.00479	1798	36	1739	21	1681	24
D8-7	1643	2496	0.658	0.10981	0.00244	4.93	0.12	0.32472	0.00374	1796	40	1807	20	1813	18
D8-10	544	750	0.725	0.10981	0.00223	4.99	0.11	0.32794	0.00353	1798	37	1818	19	1828	17
D8-11	2049	4557	0.450	0.10933	0.00186	4.86	0.08	0.32056	0.00258	1789	27	1795	15	1792	13
D8-12	1597	3983	0.401	0.10907	0.00187	5.09	0.09	0.33642	0.00265	1784	31	1835	15	1869	13
D8-13	2398	4108	0.584	0.11061	0.00208	5.23	0.13	0.34160	0.00684	1810	33	1858	21	1894	33
D8-14	1072	2053	0.522	0.10932	0.00225	5.08	0.11	0.33472	0.00462	1788	37	1833	19	1861	22
D8-15	3830	9444	0.406	0.10793	0.00207	4.37	0.08	0.29104	0.00295	1765	35	1706	16	1647	15
D8-16	2653	9097	0.292	0.10719	0.00187	4.35	0.08	0.29178	0.00329	1754	32	1702	16	1650	16
D8-17	7368	10648	0.692	0.10843	0.00180	4.26	0.08	0.28290	0.00297	1773	31	1686	15	1606	15
D8-18	1760	3435	0.512	0.10842	0.00188	4.80	0.09	0.31896	0.00285	1773	31	1785	15	1785	14
D8-20	5572	12845	0.434	0.10810	0.00227	4.23	0.09	0.28231	0.00266	1769	38	1680	18	1603	13

Table 2. Re-Os isotope data of molybdenite samples from the Zhaiwa Mo deposit

Sample	Weight, g	Brief sample description	Re, ng/g	^{187}Re, ng/g	^{187}Os, ng/g	Model age, Ma
MPG-1	0.05014	Quartz-molybdenite veinlet in granite porphyry	3419 ± 27	2149 ± 17	65.10 ± 0.39	1794 ± 25
MPG-2	0.05117	Quartz-molybdenite vein in biotite-amphibole plagiogneiss	3834 ± 32	2410 ± 20	72.63 ± 0.52	1783 ± 26
MPG-3	0.05018	Quartz-molybdenite-pyrite vein in biotite-amphibole plagiogneiss	2330 ± 15	1464 ± 9	44.22 ± 0.31	1786 ± 24
MPG-4	0.05027	Quartz-molybdenite-pyrite vein in biotite-amphibole plagiogneiss	2990 ± 18	1879 ± 11	56.71 ± 0.39	1784 ± 24
MPG-5	0.00561	Quartz-molybdenite vein in biotite-amphibole plagiogneiss	3326 ± 33	2091 ± 21	63.55 ± 0.44	1798 ± 28
HLP	0.00507	Molybdenite standard from a carbonatite vein-type Mo-Pb deposit	289266 ± 2080	181809 ± 1308	669.2 ± 4.1	220.5 ± 3.0

for Mo mineralization (Shinohara et al., 1995; Richards, 2003). This speculation is strengthened by our field observation as noted above. Moreover, the magma intrusion and Mo mineralization of Zhaiwa deposit are also coeval with the peak volcanic eruption period (1.78–1.75 Ga) in which the Xiong'er Group was formed in the EQMB (Zhao et al., 2009; He et al., 2009; Wang et al., 2010a; Cui et al., 2011). To conclude, geochronology data reported here suggests that the Mo mineralization at Zhaiwa is genetically associated with the granite porphyry; both the magma intrusion and Mo mineralization are coeval with the regional Xiong'er volcanism/magmatism during the late Paleoproterozoic.

The Re concentrations in molybdenite from the Zhaiwa porphyry Mo deposit vary between 2.33 and 3.83 ppm, with a mean of 3.18 ppm. The content of Re has been used as a proxy to indicate its sources (Mao et al., 1999; Stein et al., 2001). The range of Re content in the Zhaiwa molybdenite is comparable to those with crustal source signature. Previous work of fluid inclusion studies and H–O isotope systematics suggest that the ore-forming fluids were magmatic-hydrothermal in origin (Deng et al., 2013a). The $\delta^{34}S$ values of ores from the deposit further indicate that the S was also mainly derived from a magmatic source (Deng et al., 2013b). Additionally, the initial Sr ratio of the sulfides in Zhaiwa ($^{87}Sr/^{86}Sr = 0.70533$) is similar to that of the Xiong'er Group ($^{87}Sr/^{86}Sr = 0.70547$) and is regarded to be sourced from the crust (Deng et al., 2013b). The combined evidence indicates that the ore-forming materials of the Zhaiwa deposit are sourced from magmas, and the magmas are mainly crustal in origin.

Source of Sulfur

The sulfides in the Zhaiwa porphyry Mo deposit are dominated by molybdenite and pyrite, with minor chalcopyrite, sphalerite, galena, pyrrhotite, bismuthinite, and native bismuth, and no sulfate minerals are detected. Therefore, the S isotope composition measured from pyrite in this study approximate those of the ore-forming fluids (Ohmoto and Rye, 1979). The $\delta^{34}S$ values of pyrite from the Zhaiwa deposit display a narrow range (5.3–6.8‰), with a mean value of 6.0‰, which is slightly higher than that of typical magmatic sulfur (0 ± 3‰; Ohmoto, 1972), but compatible with that of the volcanic rocks of the Xiong'er Group (2.5–5.4‰; Fan et al., 1994) in the district, possibly indicating the same source of sulfur for the Zhaiwa Mo mineralization and Xiong'er volcanism/magmatism in this district, and that is attributed to magmatic source (Ohmoto and Rye, 1979).

Table 3. In situ LA-MC-ICP-MS sulfur isotope data of pyrite from the main mineralization stage in the Zhaiwa Mo deposit

Sample No.	$\delta^{34}S$, ‰	2SE
9ZW-1	6.1	0.1
9ZW-2	5.7	0.1
9ZW-3	5.7	0.1
9ZW-4	5.9	0.1
9ZW-5	6.3	0.2
9ZW-6	5.6	0.1
9ZW-7	5.9	0.1
9ZW-8	5.3	0.1
9ZW-9	5.9	0.1
9ZW-10	6.2	0.3
9ZW-11	5.9	0.2
9ZW-12	6.1	0.2
9ZW-13	5.9	0.3
9ZW-14	6.3	0.1
9ZW-15	6.8	0.1

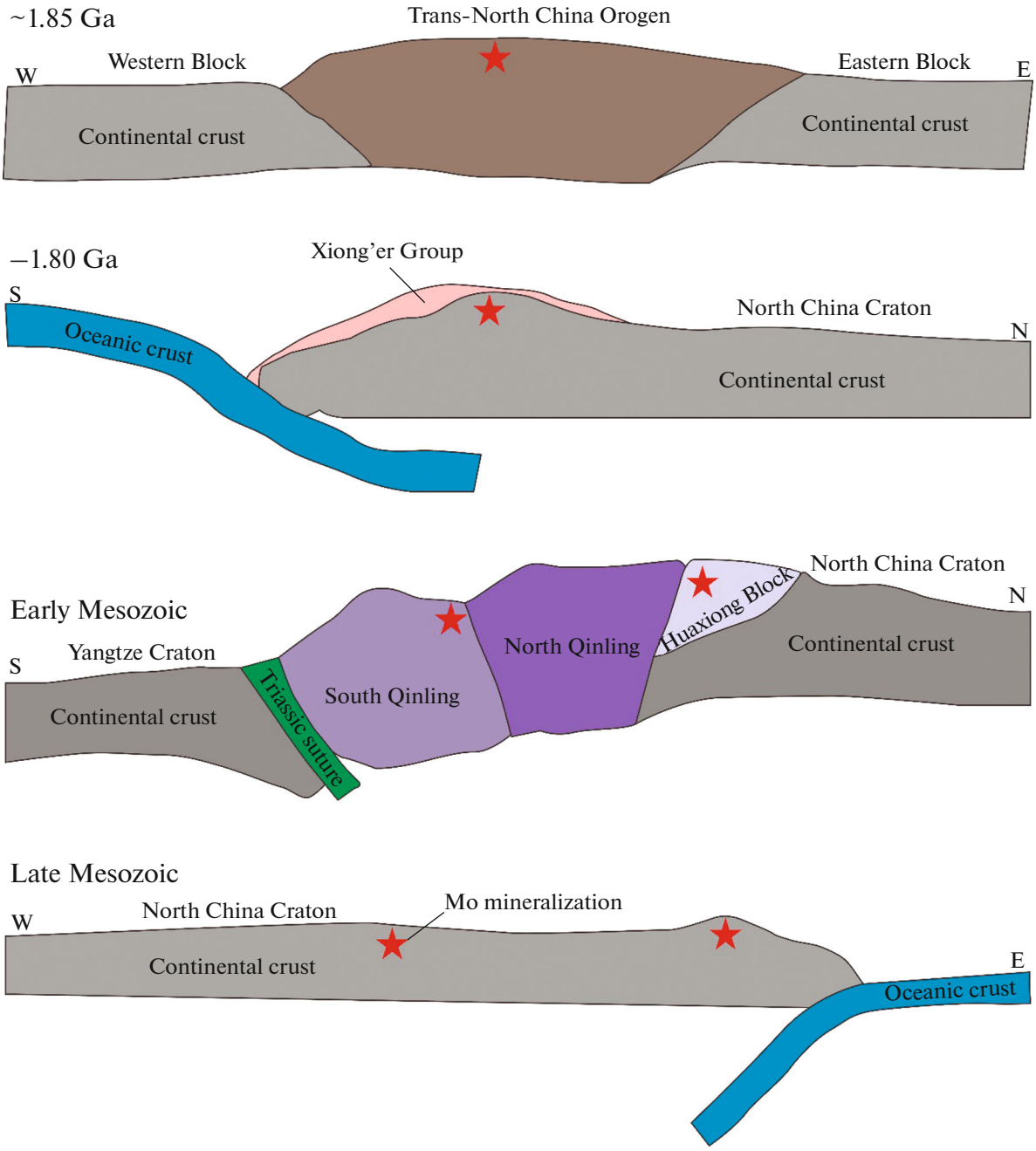

Fig. 6. Cartoons showing the Mo mineralization pulses in the EQMB and related geodynamic events (details in the text). The red star presents the Mo mineralization (modified from Mao et al., 2011; Deng et al., 2013a).

Implications on Regional Tectonic Evolution

The Xiong'er Group preserves evidence of a large volcanic event, second in size only to the event that formed the crystalline basement of the NCC. The Xiong'er Group has only experienced minor metamorphism, indicating the formation post-dates the major collisional event between the Eastern and Western Blocks within the NCC. However, the tectonic setting of the Xiong'er Group is still controversial, as noted above, with the various proposed tectonic environments including arc (Hu et al., 1988; Jia, 1987; Chen and Fu, 1992), rift (Sun et al., 1981, 1985), mantle plume (Peng et al., 2008), and flat subduction (Wang et al., 2010a). One way to resolve the question of the tectonic environment is to use mineral-system type as a constraint (Chen, 2017). Chen et al. (2017a) classified the porphyry Mo deposits in China into Climax-, Dabie- and Endako-types, and established a link between the genetic types of porphyry Mo deposits and tectonic settings including rift setting, conti-

nental collision, or magmatic arc. At the Zhaiwa area, geochronological data and field observations consistently suggest that the Zhaiwa Mo deposit is a porphyry type and formed during the late Paleoproterozoic. Cui et al. (2010, 2011, 2013) conducted detailed petrological, geochemical and geochronological work on the late Paleoproterozoic intermediate-felsic intrusive rocks in the Xiao Mountains, Xiong'er Terrane, based on which they conclude that these rocks are formed in an extensional rift setting. The synthesis of petrology, geochronology, geochemistry, and isotopes studies revealed that the Xiong'er volcanic rocks may have been generated from the high-degree partial melting of late Archean subduction-modified lithospheric mantle in a post-orogenic extensional setting (Wang et al., 2010a). Combining the findings of our study and previous work, we speculate that the tectonic setting of the formation of Zhaiwa Mo deposit during the late Paleoproterozoic is an extensional setting, rather than an arc setting.

Based on the correlation of mineral-system and tectonic environment, we therefore propose the regional tectonic evolution for EQMB as follows (Fig. 6). Li et al. (2011a) reported the 1.85 Ga Longmengdian quartz-vein type Mo deposit in the Xiong'er Terrane of the EQMB, is coeval with the final amalgamation between an Eastern and a Western Blocks, which was achieved at ca 1.85 Ga (Zhao et al., 2001, 2007; Guo and Zhai, 2001; Liu et al., 2011). During this period, the old basement experienced extensive re-working. The ore-forming metals such as Mo were remobilized, redistributed and enriched in the ore-forming fluids forming the Longmendian quartz-vein type deposits. Thereafter the tectonic stress field changed from compression to extension. The extensional setting has induced the eruption of the Xiong'er volcanic rocks and the late Paleoproterozoic intrusions, together with the Zhaiwa porphyry Mo mineralization. From the late Paleoproterozoic onwards, most of the Mo deposits in the EQMB are related to the Mesozoic porphyry/skarn systems (Hu et al., 1988; Stein et al., 1997; Chen et al., 2000; Zhou et al., 2020; Hu et al., 2022). Driven by the continental collision between the NCC and Yangtze Craton the early Mesozoic (mostly Triassic and minor Early Jurassic) Mo mineralization was formed and mainly derived from crustal magmatic sources (Gao et al., 2010; Wang et al., 2010a; Li et al., 2011a; Deng et al., 2016). When the time evolved to the late Mesozoic (Late Jurassic–Early Cretaceous), the tectonic setting was mainly controlled by the westward subduction of the Paleo-Pacific plate, during which another significant episode of Mo mineralization occurred (Zeng et al., 2013; Chen et al., 2000; Mao et al., 2008, 2011).

Significance to Regional Exploration in the EQMB

Existing molybdenite Re–Os ages show that the Mo mineralization in the EQMB was formed concentrating in three periods (Fig. 6): the late Paleoproterozoic (1.85–1.76 Ga) (Deng et al., 2009; Li et al., 2009; Li et al., 2011a), the early Mesozoic (mostly Triassic and minor Early Jurassic) (Gao et al., 2010; Wang et al., 2010b; Li et al., 2011b; Deng et al., 2016), and the late Mesozoic (Late Jurassic–Early Cretaceous (Chen et al., 2000; Mao et al., 2008, 2011; Liu et al., 2021). These ages correspond to the Xiongerian, Indosinian, and Yanshanian mineralization events, respectively. Most of the Mo deposits in the EQMB are associated with Mesozoic porphyry/skarn systems and have been extensively studied (Hu et al., 1988; Stein et al., 1997; Chen et al., 2000; Zhou et al., 2020; Hu et al., 2022). This study, in combination with several others (Deng et al., 2009; Li et al., 2009, 2011a) have extended the known age range of mineralization, and highlight the importance of the porphyry Mo mineralization system during the late Paleoproterozoic, in particular, those associated with the Xiong'er volcanism/magmatism. Coincidently, the stratigraphic unit (e.g., Xiong'er Group) would be the main contributor of Mo metal for the late Paleoproterozoic Mo mineralization in the EQMB (Li et al., 2023). Future exploration work could consider targeting the Archean hypometamorphic rocks for prospecting the late Paleoproterozoic Mo mineralization, such as the Xiong'er Group and Taihua Supergroup.

CONCLUSIONS

The molybdenite Re-Os isochron dating indicates a mineralization age of 1794 ± 45 Ma for the Zhaiwa deposit. Zircon U-Pb dating indicates an emplacement age of 1791 ± 16 Ma for the host granite porphyry. In situ S isotope analysis of pyrite indicate that the S may have derived from a magmatic source. The Zhaiwa deposit can be certainly classified as a porphyry Mo deposit, and its formation was related to the Xiong'er volcanism during the late Paleoproterozoic in an extensional setting. The late Paleoproterozoic Mo mineralization is a significant metallogenic event in the EQMB, providing a target for future exploration in the region.

ACKNOWLEDGMENTS

We would like to thank Drs. Xiaohua Deng and Lingli Zhou for help in improving the manuscript. We are grateful to Associate Editor Dr. A.B. Kuznetsov, and reviewers B.V. Belyatsky, and Huan Li for detailed comments in improving the manuscript. Finally, thanks to Drs. Peiwen Chen and Shaoxiong Chu for contribution to field work.

FUNDING

This work was supported by the National Key Research and Development Program of China (No. 2021YFC2901805) and Geological Surveying Project of China Geological Survey (Nos. DD20230355, DD20230356).

CONFLICT OF INTEREST

The authors of this work declare that they have no conflicts of interest.

REFERENCES

F. Barra, J. Ruiz, R. Mathur, and S. Titley, "A Re–Os study of sulfide minerals from the Bagdad porphyry Cu–Mo deposit, northern Arizona, USA," Mineral. Deposita **38** (5), 585–596 (2003). https://doi.org/10.1007/s00126-002-0341-0

J. M. Brenan, D. J. Cherniak, and L. A. Rose, "Diffusion of osmium in pyrrhotite and pyrite: implications for closure of the Re–Os isotopic system," Earth Planet. Sci. Lett. **180** (3–4), 399–413 (2000). https://doi.org/10.1016/s0012-821x(00)00165-5

Y. J. Chen, "Orogenic-type deposits and their metallogenic model and exploration potential," Geol. China **33**, 1181–1196 (2006).

Y. J. Chen and S. G. Fu, *Gold Mineralization in West Henan, China* (Seismological Press, Beijing, 1992).

Y. J. Chen and Y. C. Zhao, "Geochemical characteristics and evolution of REE in the Early Precambrian sediments: evidence from the southern margin of the North China Craton," Episodes **20**, 109–116 (1997).

Ya. Chen, C. Li, J. Zhang, Z. Li, and H. Wang, "Sr and O isotopic characteristics of porphyries in the Qinling molybdenum deposit belt and their implication to genetic mechanism and type," Sci. China Ser. D: Earth Sci. **43** (S1), 82–94 (2000). https://doi.org/10.1007/bf02911935

Ya. Chen, F. Pirajno, and Yi. Sui, "Isotope geochemistry of the Tieluping silver-lead deposit, Henan, China: A case study of orogenic silver-dominated deposits and related tectonic setting," Mineral. Deposita **39** (5–6), 560–575 (2004). https://doi.org/10.1007/s00126-004-0429-9

Ya. Chen, F. Pirajno, J. Qi, J. Li, and H. Wang, "Ore Geology, Fluid Geochemistry and Genesis of the Shanggong Gold Deposit, Eastern Qinling Orogen, China," Resour. Geol. **56** (2), 99–116 (2006). https://doi.org/10.1111/j.1751-3928.2006.tb00272.x

Ya. Chen, F. Pirajno, N. Li, D. Guo, and Yo. Lai, "Isotope systematics and fluid inclusion studies of the Qiyugou breccia pipe-hosted gold deposit, Qinling Orogen, Henan province, China: Implications for ore genesis," Ore Geol. Rev. **35** (2), 245–261 (2009). https://doi.org/10.1016/j.oregeorev.2008.11.003

Ya. Chen, F. Pirajno, N. Li, and X. Deng, "Molybdenum deposits in China," Ore Geol. Rev. **81**, 401–404 (2017). https://doi.org/10.1016/j.oregeorev.2016.11.002

Ya. Chen, P. Wang, N. Li, Yo. Yang, and F. Pirajno, "The collision-type porphyry Mo deposits in Dabie Shan, China," Ore Geol. Rev. **81**, 405–430 (2017). https://doi.org/10.1016/j.oregeorev.2016.03.025

Ya. Chen, C. Zhang, P. Wang, F. Pirajno, and N. Li, "The Mo deposits of Northeast China: A powerful indicator of tectonic settings and associated evolutionary trends," Ore Geol. Rev. **81**, 602–640 (2017). https://doi.org/10.1016/j.oregeorev.2016.04.017

M. L. Cui, B. L. Zhang, P. Peng, L. C. Zhang, X. L. Shen, Z. H. Guo, and X. F. Huang, "Zircon/baddeleyite U-Pb dating for the Paleoproterozoic intermediate–acid intrusive rocks in Xiaoshan Mountains, west of Henan Province and their constraints on the age of the Xiong'er Volcanic Province," Acta Petrol. Sin **26**, 1541–1549 (2010).

M. Cui, B. Zhang, and L. Zhang, "U–Pb dating of baddeleyite and zircon from the Shizhaigou diorite in the southern margin of North China Craton: Constrains on the timing and tectonic setting of the Paleoproterozoic Xiong'er group," Gondwana Res. **20** (1), 184–193 (2011). https://doi.org/10.1016/j.gr.2011.01.010

M. Cui, L. Zhang, B. Zhang, and M. Zhu, "Geochemistry of 1.78 Ga A-type granites along the southern margin of the North China Craton: implications for Xiong'er magmatism during the break-up of the supercontinent Columbia," Int. Geol. Rev. **55** (4), 496–509 (2013). https://doi.org/10.1080/00206814.2012.736709

X. H. Deng, Y. J. Chen, J. M. Yao, W. B. Li, N. Li, Y. Wang, M. Mi, and Y. Zhang, Geol. China **35**, 1250–1266 (2008).

X. Deng, Ya. Chen, M. Santosh, J. Yao, and Ya. Sun, "Re–Os and Sr–Nd–Pb isotope constraints on source of fluids in the Zhifang Mo deposit, Qinling Orogen, China," Gondwana Res. **30**, 132–143 (2009). https://doi.org/10.1016/j.gr.2015.02.020

X. H. Deng, Y. J. Chen, M. Santosh, and J. M. Yao, "Genesis of the 1.76Ga Zhaiwa Mo–Cu and its link with the Xiong'er volcanics in the North China Craton: Implications for accretionary growth along the margin of the Columbia supercontinent," Precambrian Res. **227**, 337–348 (2013). https://doi.org/10.1016/j.precamres.2012.02.014

X. H. Deng, Y. J. Chen, M. Santosh, G. C. Zhao, and J. M. Yao, "Metallogeny during continental outgrowth in the Columbia supercontinent: Isotopic characterization of the Zhaiwa Mo–Cu system in the North China Craton," Ore Geol. Rev. **51**, 43–56 (2013). https://doi.org/10.1016/j.oregeorev.2012.11.004

X. H. Deng, Ya. Chen, M. Santosh, J. Yao, and Ya. Sun, "Re–Os and Sr–Nd–Pb isotope constraints on source of fluids in the Zhifang Mo deposit, Qinling Orogen, China," Gondwana Res. **30**, 132–143 (2016). https://doi.org/10.1016/j.gr.2015.02.020

Yu. Dong, J. Genser, F. Neubauer, G. Zhang, X. Liu, Z. Yang, and B. Heberer, "U-Pb and 40Ar/39Ar geochronological constraints on the exhumation history of the North Qinling terrane, China," Gondwana Res. **19** (4), 881–893 (2011). https://doi.org/10.1016/j.gr.2010.09.007

A. Du, S. Wu, D. Sun, S. Wang, W. Qu, R. Markey, H. Stain, J. Morgan, and D. Malinovskiy, "Preparation and Certification of Re-Os Dating Reference Materials: Molybdenites HLP and JDC," Geostand. Geoanalyt. Res. **28** (1), 41–52 (2004). https://doi.org/10.1111/j.1751-908x.2004.tb01042.x

H. R. Fan, Y. H. Xie, R. Zhao, and Y. L. Wang, "Stable isotope geochemistry of rocks and gold deposits in Xion'ershan area, Western Henan," Collect. Geol. Explor. **9**, 54–64 (1994).

H. R. Fan, Y. H. Xie, X. Z. Zheng, and Y. L. Wang, "Ore-forming fluids in hydrothermal breccia-related gold mineralization in Qiyugou, Henan Province," Acta Petrol. Sin **16**, 559–563 (2000).

H. Fan, F. Hu, S. A. Wilde, K. Yang, and C. Jin, "The Qiyugou gold-bearing breccia pipes, Xiong'ershan region, central China: fluid-inclusion and stable-isotope evidence for an origin from magmatic fluids," Int. Geol. Rev. **53** (1), 25–45 (2011). https://doi.org/10.1080/00206810902875370

J. Feng, L. Tang, B. Yang, M. Santosh, S. Zhang, B. Xu, S. Won Kim, and Yu. Sheng, "Bastnäsite U-Th-Pb age, sulfur isotope and trace elements of the Huangshui'an deposit: Implications for carbonatite-hosted Mo-Pb-REE mineralization in the Qinling Orogenic Belt, China," Ore Geol. Rev. **143**, 104790 (2022). https://doi.org/10.1016/j.oregeorev.2022.104790

Ya. Gao, H. Ye, J. Mao, and Yo. Li, "Geology, geochemistry and genesis of the Qianfanling quartz-vein Mo deposit in Songxian County, Western Henan Province, China," Ore Geol. Rev. **55**, 13–28 (2010). https://doi.org/10.1016/j.oregeorev.2013.04.005

J. Guo and M. Zhai, "Sm-Nd age dating of high-pressure granulites and amphibolite from Sanggan area, North China craton," Chin. Sci. Bull. **46** (2), 106–111 (2001). https://doi.org/10.1007/bf03187002

Yi. Han, S. Zhang, F. Pirajno, Yu. Wang, and Yu. Zhang, "New 40Ar–39Ar age constraints on the deformation along the Machaoying fault zone: Implications for Early Cambrian tectonism in the North China Craton," Gondwana Res. **16** (2), 255–263 (2009). https://doi.org/10.1016/j.gr.2009.02.001

Y. H. He, G. C. Zhao, M. Sun, and X. P. Xia, "SHRIMP and LA-ICP-MS zircon geochronology of the Xiong'er volcanic rocks: Implications for the Paleo-Mesoproterozoic evolution of the southern margin of the North China Craton," Precambrian Res. **168** (3-4), 213–222 (2009). https://doi.org/10.1016/j.precamres.2008.09.011

P. W. O. Hoskin and L. P. Black, "Metamorphic zircon formation by solid-state recrystallization of protolith igneous zircon," J. Metamorphic Geol. **18** (4), 423–439 (2000). https://doi.org/10.1046/j.1525-1314.2000.00266.x

S. X. Hu, Q. L. Lin, Z. M. Chen, and S. M. Li, *Geology and metallogeny of the collision belt between the North and the South China plates* (Nanjing University Press, Nanjing, 1988).

X. Hu, S. Zhang, T. Tsunogae, L. Tang, W. Li, Yu. Sheng, and J. Feng, "Genesis and magmatic-hydrothermal evolution of the Shapoling Mo deposit, East Qinling, China: Insights from geochronology, petrogenesis and fluid evolution," Ore Geol. Rev. **143**, 104789 (2022). https://doi.org/10.1016/j.oregeorev.2022.104789

C. Z. Jia, "Geochemistry and tectonics of the Xionger Group in the eastern Qinling Mountains of China-a mid-Proterozoic volcanic arc related to plate subduction," in *Geochemistry and Mineralization of Proterozoic Volcanic Suites*, Ed. by T. C. Pharaoh, R. D. Beckinsale, and D. Rickard (Geol. Soc. London Spec. Publ., 1987), Vol. 33, pp. 437–448.

R. V. Kirkham, "Porphyry deposits," in *Report of Activities: Part B. Geological Survey of Canada*, Ed. by R. G. Blackadar (Geol. Surv. Canada, Ottawa, 1972), pp. 62–64.

A. Kröner, W. Compston, Z. Guo-Wei, G. An-Lin, and W. Todt, "Age and tectonic setting of Late Archean greenstone-gneiss terrain in Henan Province, China, as revealed by single-grain zircon dating," Geology **16** (3), 211–215 (1988). https://doi.org/10.1130/0091-7613(1988)016<0211:aatsol>2.3.co;2

F. Li, R. Mathur, J. Li, N. Li, X. Deng, Yi. Yao, T. Zhao, and J. Yao, "Link Mo isotopes to the sources of the Paleoproterozoic Mo mineralization in the Qinling orogen," Ore Geol. Rev. **160**, 105618 (2023). https://doi.org/10.1016/j.oregeorev.2023.105618

H. M. Li, Y. C. Chen, H. S. Ye, D. H. Wang, B. J. Guo, and Y. F. Li, "Mo, (W), Au, Ag, Pb, Zn minerogenetic series related to Mesozoic magmatic activities in the East Qinling-Dabie Mountains," Acta Geol. Sin. **82**, 1468–1477 (2008).

H. M. Li, H. S. Ye, D. H. Wang, Y. C. Chen, W. J. Qu, and A. D. Du, "Re-Os dating of molybdenites from Zhaiwa Mo deposit in Xiong'er Mountain, western Henan Province, and its geological significance," Miner. Deposits **28**, 133–142 (2009).

N. Li, Y. J. Chen, H. Zhang, T. P. Zhao, X. H. Deng, Y. Wang, and Z. Y. Ni, "Molybdenum deposits in East Qinling," Earth Sci. Front. **14**, 186–198 (2007).

N. Li, Ya. Chen, I. R. Fletcher, and Q. Zeng, "Triassic mineralization with Cretaceous overprint in the Dahu Au–Mo deposit, Xiaoqinling gold province: Constraints from SHRIMP monazite U–Th–Pb geochronology," Gondwana Res. **20** (2–3), 543–552 (2011). https://doi.org/10.1016/j.gr.2010.12.013

N. Li, Y. J. Chen, M. Santosh, J. M. Yao, Y. L. Sun, and J. Li, "The 1.85 Ga Mo mineralization in the Xiong'er Terrane, China: Implications for metallogeny associated with assembly of the Columbia supercontinent," Precambrian Res. **186** (1–4), 220–232 (2011). https://doi.org/10.1016/j.precamres.2011.01.019

N. Li, E. J. M. Carranza, Z. Ni, and D. Guo, "The CO_2-rich magmatic-hydrothermal fluid of the Qiyugou breccia pipe, Henan Province, China: implication for breccia genesis and gold mineralization," Geochem.: Explor., Environ., Anal. **12** (2), 147–160 (2012). https://doi.org/10.1144/1467-7873/10-mindep-057

C. Liu, G. Zhao, M. Sun, F. Wu, J. Yang, C. Yin, and W. H. Leung, "U–Pb and Hf isotopic study of detrital zircons from the Yejishan Group of the Lüliang Complex: Constraints on the timing of collision between the Eastern and Western Blocks, North China Craton," Sedimentary Geol. **236** (1-2), 129–140 (2011). https://doi.org/10.1016/j.sedgeo.2011.01.001

G. R. Liu, G. J. Zhang, F. J. Jiang, X. D. Ding, Y. J. Sun, J. Sun, and E. Ma, "Nanostructured high-strength molybdenum alloys with unprecedented tensile ductility," Nat. Mater. **12** (4), 344–350 (2013). https://doi.org/10.1038/nmat3544

L. E. Liu, G. M. Hu, and F. Q. Zhi, "Control of Zhaiwa concealed mass of rock on peripheral silver polymetallic deposits in West Henan," Miner. Resour. Geol **18**, 31–34 (2004).

Q. Liu, H. Li, Yo. Shao, M. Bala Girei, W. Jiang, H. Yuan, and X. Zhang, "Age, genesis, and tectonic setting of the Qiushuwan Cu–Mo deposit in East Qinling (Central China): Constraints from Sr–Nd–Hf isotopes, zircon U–Pb and molybdenite Re–Os dating," Ore Geol. Rev. **132**, 103998 (2021). https://doi.org/10.1016/j.oregeorev.2021.103998

Y. S. Liu, S. Gao, Z. C. Hu, C. G. Gao, K. Q. Zong, and D. B. Wang, "Continental and oceanic crust recycling-induced melt-peridotite interactions in the Trans-North China Orogen: U-Pb dating, Hf isotopes and trace elements in zircons from mantle xenoliths," J. Petrol. **51** (1–2), 537–571 (2010). https://doi.org/10.1093/petrology/egp082

K. R. Ludwig, *User's Manual for Isoplot 3.00, a Geochronological Toolkit for Microsoft Excel* (Berkeley Geochronol. Center, Spec. Publ., 2003).

J. Mao, R. Goldfarb, Z. Zhang, W. Xu, Yu. Qiu, and J. Deng, "Gold deposits in the Xiaoqinling–Xiong'ershan region, Qinling Mountains, central China," Mineral. Deposita **37** (3-4), 306–325 (2002). https://doi.org/10.1007/s00126-001-0248-1

J. W. Mao, Z. C. Zhang, Z. H. Zhang, and A. D. Du, "Re-Os isotopic dating of molybdenite in the Xiaoliugou W (Mo) deposit in the northern Qilian Mountain and its geological significance," Geochim. Cosmochim. Acta **63**, 1815–1818 (1999).

J. W. Mao, G. Q. Xie, F. Bierlein, W. J. Qü, A. D. Du, H. S. Ye, F. Pirajno, H. M. Li, B. J. Guo, Y. F. Li, and Z. Q. Yang, "Tectonic implications from Re–Os dating of Mesozoic molybdenum deposits in the East Qinling–Dabie orogenic belt," Geochimica Cosmochim. Acta **72** (18), 4607–4626 (2008). https://doi.org/10.1016/j.gca.2008.06.027

J. W. Mao, F. Pirajno, J. F. Xiang, J. J. Gao, H. S. Ye, Y. F. Li, and B. J. Guo, "Mesozoic molybdenum deposits in the east Qinling–Dabie orogenic belt: Characteristics and tectonic settings," Ore Geol. Rev. **43** (1), 264–293 (2011). https://doi.org/10.1016/j.oregeorev.2011.07.009

H. Ohmoto, "Systematics of sulfur and carbon isotopes in hydrothermal ore deposits," Econ. Geol. **67** (5), 551–578 (1972). https://doi.org/10.2113/gsecongeo.67.5.551

H. Ohmoto and R. O. Rye, "Isotopes of sulfur and carbon," in *Geochemistry of Hydrothermal Ore Deposits*, Ed. by H. L. Barnes (Wiley, New York, 1979), pp. 509–567.

P. Peng, M. Zhai, R. E. Ernst, J. Guo, F. Liu, and B. Hu, "A 1.78 Ga large igneous province in the North China craton: The Xiong'er volcanic province and the North China dyke swarm," Lithos **101** (3-4), 260–280 (2008). https://doi.org/10.1016/j.lithos.2007.07.006

Z. Qian, F. Yang, W. Ren, M. Santosh, J. Liu, H. Li, and F. Xue, "Two episodes of Mesozoic granitic magmatism in East Qinling, central China: Constraints from geochemistry and isotope geochronology of the Huangbeiling pluton," Lithos **454-455**, 107234 (2023). https://doi.org/10.1016/j.lithos.2023.107234

J. P. Richards, "Tectono-magmatic precursors for porphyry Cu–(Mo–Au) deposit formation," Econ. Geol. **98** (8), 1515–1533 (2003). https://doi.org/10.2113/98.8.1515

J. A. Shields, Jr, and E. L. Baker, "Molybdenum alloys and emerging applications," Adv. Mater. Processes **155**, 61 (1999).

H. Shinohara, K. Kazahaya, and J. B. Lowenstern, "Volatile transport in a convecting magma column: Implications for porphyry Mo mineralization," Geology **23** (12), 1091 (1995). https://doi.org/10.1130/0091-7613(1995)023<1091:vti-acm>2.3.co;2

M. I. Smoliar, R. J. Walker, and J. W. Morgan, "Re-Os ages of group IIA, IIIA, IVA, and IVB iron meteorites," Science **271** (5252), 1099–1102 (1996). https://doi.org/10.1126/science.271.5252.1099

H. J. Stein, R. J. Markey, J. W. Morgan, A. Du, and Y. Sun, "Highly precise and accurate Re-Os ages for molybdenite from the East Qinling molybdenum belt, Shaanxi Province, China," Econ. Geol. **92** (7-8), 827–835 (1997). https://doi.org/10.2113/gsecongeo.92.7-8.827

H. J. Stein, K. Sundblad, R. J. Markey, J. W. Morgan, and G. Motuza, "Re-Os ages for Archean molybdenite and pyrite, Kuittila-Kivisuo, Finland and Proterozoic molybdenite, Kabeliai, Lithuania: testing the chronometer in a metamorphic and metasomatic setting," Mineral. Deposita **33** (4), 329–345 (1998). https://doi.org/10.1007/s001260050153

H. J. Stein, R. J. Markey, J. W. Morgan, J. L. Hannah, and A. Scherstén, "The remarkable Re–Os chronometer in molybdenite: how and why it works," Terra Nova **13** (6), 479–486 (2001). https://doi.org/10.1046/j.1365-3121.2001.00395.x

K. Suzuki, H. Shimizu, and A. Masuda, "Re-Os dating of molybdenites from ore deposits in Japan: Implication for the closure temperature of the Re-Os system for molybdenite and the cooling history of molybdenum ore deposits," Geochim. Cosmochim. Acta **60** (16), 3151–3159 (1996). https://doi.org/10.1016/0016-7037(96)00164-0

S. Sun, B. L. Cong, and J. L. Li, "Meso-Neoproterozoic sedimentary basins in Henan and Shanxi Provinces," Sci. Geol. Sin **16**, 314–322 (1981).

S. Sun, G. W. Zhang, and Z. M. Chen, *Geologic Evolution of the South of the North China Fault-Block* (China Metallurgical Industry Press, Beijing, 1985).

X. Wang, S. Jiang, and B. Dai, "Melting of enriched Archean subcontinental lithospheric mantle: Evidence from the ca. 1760Ma volcanic rocks of the Xiong'er Group, southern margin of the North China Craton," Precambrian Res. **182** (3), 204–216 (2010). https://doi.org/10.1016/j.precamres.2010.08.007

Yo. Wang, P. Feng, L. Zhou, and Q. Zeng, "Genetic links of porphyry Mo-epithermal Pb–Zn–Ag mineralization system: a case study of the Shipingchuan polymetallic deposit, South China," Acta Geochimica **41** (2), 307–323 (2022). https://doi.org/10.1007/s11631-022-00530-5

Y. T. Wang, H. S. Ye, A. W. Ye, Y. G. Li, Y. Shuai, C. Q. Zhang, and J. Z. Dai, "Re-Os age of molybdenite from the Majiawa Au-Mo deposit of quartz vein type in the north margin of the Xiaoqinling gold area and its implication for metallogeny," Earth Sci. Front, 140–145 (2010).

Z. G. Wang, H. Cui, and M. L. Xu, *Tectonic Evolution and Mineralization of the Southern Margin of the North China Block* (China Metallurgical Industry Press, Beijing, 1997).

Ya. Wu, Ya. Chen, and K. Zhou, "Mo deposits in Northwest China: Geology, geochemistry, geochronology and tectonic setting," Ore Geol. Rev. **81**, 641–671 (2017). https://doi.org/10.1016/j.oregeorev.2016.07.010

C. F. Xie, C. Y. Xiong, N. Hu, and J. S. Li, "A study on regional metallogenic regularity of the East Qinling-Dabie orogenic belt," Geol. Miner. Resour. S. China **3**, 14–22 (2001).

L. W. Xue, Z. L. Yuan, and Y. S. Zhang, "The Sm-Nd isotope age of Taihua group in Lushan area and their implications," Geochimica **24**, 92–97 (1995).

Q. Z. Yang, S. L. Peng, S. W. Zhang, and L. E. Liu, "Geological characteristics and ore-forming prospect of Zhai'ao copper ore of porphyry type in West Henan," Geol. Miner. Resour. Res, 43–46 (2003a).

Q. Z. Yang, L. X. Zhang, S. L. Peng, and J. Q. Lai, "Geochemical characteristics and prospecting direction of Zhai'ao region," Western Henan. Miner. Resour. Geol. **17**, 458–460 (2003b).

Yo. Yang and P. Wang, "Geology, geochemistry and tectonic settings of molybdenum deposits in Southwest China: A review," Ore Geol. Rev. **81**, 965–995 (2017). https://doi.org/10.1016/j.oregeorev.2016.10.017

B. Yu, Q. Zeng, H. E. Frimmel, W. Chen, M. Ren, G. Huang, J. Wu, W. Xie, L. Zhou, J. Yang, and J. Xue, "Genesis of the Shirengou gold deposit, northern North China Craton, based on zircon U-Pb, fluid inclusion, sulfide compositional and S isotope data," J. Geochem. Explor. **256**, 107358 (2024). https://doi.org/10.1016/j.gexplo.2023.107358

Q. Zeng, J. Liu, K. Qin, H. Fan, S. Chu, Yo. Wang, and L. L. L. Zhou, "Types, characteristics, and time–space distribution of molybdenum deposits in China," Int. Geol. Rev. **55** (11), 1311–1358 (2013). https://doi.org/10.1080/00206814.2013.774195

G. Zhao, S. A. Wilde, P. A. Cawood, and M. Sun, "Archean blocks and their boundaries in the North China Craton: lithological, geochemical, structural and P–T path constraints and tectonic evolution," Precambrian Res. **107** (1–2), 45–73 (2001). https://doi.org/10.1016/s0301-9268(00)00154-6

G. Zhao, A. Kröner, S. A. Wilde, M. Sun, S. Li, X. Li, J. Zhang, X. Xia, and Ya. He, "Lithotectonic elements and geological events in the Hengshan–Wutai–Fuping belt: a synthesis and implications for the evolution of the Trans-North China Orogen," Geol. Mag. **144** (5), 753–775 (2007). https://doi.org/10.1017/s0016756807003561

G. Zhao, Ya. He, and M. Sun, "The Xiong'er volcanic belt at the southern margin of the North China Craton: Petrographic and geochemical evidence for its outboard position in the Paleo-Mesoproterozoic Columbia supercontinent," Gondwana Res. **16** (2), 170–181 (2009). https://doi.org/10.1016/j.gr.2009.02.004

G. Zhang, Yu. Bai, Yo. Sun, A. Guo, D. Zhou, and T. Li, "Composition and evolution of the archaean crust in central Henan, China," Precambrian Res. **27** (1–3), 7–35 (1985). https://doi.org/10.1016/0301-9268(85)90004-x

G. W. Zhang, B. R. Zhang, X. C. Yuan, and Q. H. Xiao, *Qinling Orogenic Belt and Continental Dynamics* (Science Press, Beijing, 2001).

D. Hou, J. Wang, D. Qu, Z. Luan, and X. Ren, "Fabrication and characterization of hydrophobic PVDF hollow fiber membranes for desalination through direct contact membrane distillation," Sep. Purif. Technol. **69** (1), 78–86 (2012). https://doi.org/10.1016/j.seppur.2009.06.026

L. M. Zhou, B. Y. Gao, L. B. Wang, C. Li, W. J. Qu, Z. Q. Hou, and A. D. Du, "Improvements on the separation method of osmium by direct distillation in Carius tube," Rock. Min. Analyt. **31**, 413–418 (2012).

T. Zhou, Q. Zeng, S. Gao, S. Chu, and J. Yang, "Geochronology, geochemistry and fluid inclusions of the Yechangping giant porphyry-skarn Mo-W deposit, East Qinling, China," Ore Geol. Rev. **127**, 103823 (2020). https://doi.org/10.1016/j.oregeorev.2020.103823

Publisher's Note. Pleiades Publishing remains neutral with regard to jurisdictional claims in published maps and institutional affiliations.